Molecular-dynamics simulations of hydrogen diffusion in niobium: Influence of imperfections

B. Roux, H. Jaffrezic, A. Chevarier, N. Chevarier, and M. T. Magda*
Institut de Physique Nucléaire de Lyon, IN2P3-CNRS et Université Claude Bernard 43, Bd. du 11 Novembre 1918, 69622 Villeurbanne Cedex, France
(Received 19 May 1994; revised manuscript received 1 December 1994)

The trapping mechanism of hydrogen in niobium has been investigated within the molecular-dynamics approach. Simulations of the diffusion process of this impurity were performed in which Nb-Nb interaction was described by an N-body potential. The potential parameters were adjusted with respect to static and dynamic properties of a Nb crystal. Nb-H interaction was represented by a two-body potential. The Arrhenius diagram of the H diffusion coefficient obtained by molecular dynamics in the single-crystal case provides too small values of activation energy in comparison with experimental data. However, molecular-dynamics simulations indicate a large increase of these values in the presence of defects. The influence of imperfections on the diffusion of hydrogen becomes less important at around 1000 K. This conclusion confirms the experimental results revealing a good characteristic (Q value $> 10^{10}$) of superconducting cavities after thermal treatments.

I. INTRODUCTION

Superconducting radio-frequency cavities were chosen for most of the future particle accelerators. In the case of pure niobium cavities, several laboratories have observed a degradation of superconducting properties related to the conditions of the cooling down process.[1-3] This effect seems to stem from hydrogen contamination which occurs during surface treatments. The influence of dissolved hydrogen on the rf breakdown field has been investigated experimentally.[4] These effects can be ascribed to the phase transition occurring in the Nb-H systems during the cooling procedure.[5] The only solution adopted so far to overcome this loss of rf superconducting properties is a high-temperature (up to 1000 K) anneal in a UHV furnace. The empirical procedure of increasing the temperature up to 1000 K in order to assure the H out diffusion is at variance with the high diffusion coefficient of hydrogen.[6] The exceptional characteristics of hydrogen in metal, namely, its large diffusion coefficient values (order of magnitude 10^{-5} cm^2 s^{-1}), and its strong dispersion depending on metal defects and impurities have been widely investigated with respect to statistics and thermodynamics[7,8] (for reviews see Völkl and Alefeld,[6] Fukai and Sugimoto,[9] and references therein). In recent years, molecular-dynamics (MD) computer simulations have emerged as a practical tool for studying the entire history of contaminant hopping in a metal. MD calculations were first performed by Gillan[10,11] in order to simulate the diffusion coefficients and activation energies of H in Nb over a large temperature range, and ultimately to pinpoint the low-temperature region where quantum corrections have to be included. Complementary work was performed later[12,13] for the case of H hopping in Pd at high temperatures, i.e., higher than the Debye temperature, Θ_D, for which a classical approach is adequate. We have used MD simulations to explore hydrogen contamination of niobium crystal. Alternatively, we have measured the influence of various surface treatments on hydrogen concentration profiling of the near surface region (the first 200 nm). Both theoretical and experimental investigations have been presented in detail in Ref. 14.

In this work we show results of the study concerning the influence of Nb crystal defects on hydrogen hopping using MD simulations of H diffusion in niobium at a temperature higher than θ_D. We first present (Sec. II) MD simulations of the Nb crystal, in which the Nb-Nb potential has been chosen to reproduce static and dynamic properties of the crystal. In Sec. III the Nb-H interaction is described by a two-body potential. The simulations show that most of the jumps are essentially those from a tetrahedral site (T) to the nearest-neighbor T sites and that the features of correlated jumps vary with temperature. Section IV is devoted to MD calculation of a diffusion coefficient of hydrogen in a Nb crystal, considering the effect of imperfections and its evolution with temperature.

II. MD SIMULATION OF NIOBIUM CRYSTAL

A. The model

We have to first model the energy of the Nb crystal as a function of position of the atoms. As we are dealing with a transition metal, a two-body potential model cannot give a good description of the crystal.[15-17] In the Nb case, Finnis and Sinclair (FS) have described an N-body potential[18] which allows us to account for the influence of neighboring atoms. Using the FS potential the total energy U of the metal system can be written as

$$U = U_P + U_N \ . \tag{1}$$

The first term U_P takes into account the binary interaction

$$U_P = \tfrac{1}{2} \sum_{i,j} V_{\mathrm{FS}}(r_{ij}) \ , \tag{2}$$

where

$$V_{FS}(r)=(r-c)^2(c_0+c_1r+c_2r^2), \quad r<c \tag{3}$$

$$V_{FS}(r)=0, \quad r\geq c. \tag{4}$$

The second term U_N which takes into account the characteristics of the transition metal is written as

$$U_N=-\sum_i \left[\sum_{j\neq i}\Phi_{FS}(r_{ij})\right]^{1/2}, \tag{5}$$

in which the sum runs over all atoms and where

$$\Phi_{FS}(r)=A^2(r-d)^2, \quad r<d \tag{6}$$

$$\Phi_{FS}(r)=0, \quad r\geq d\ . \tag{7}$$

The function in brackets from Eq. (5) involves a sum of pair terms, and its square-root form can be interpreted as a density function in the sense of the embedded atom model of Daw and Baskes.[19] The functions $V(r)$ and $\Phi_{FS}(r)$ are polynomials cut off at some chosen distances c and d which can be adjusted to stay between a and $\sqrt{2}a$ (a being the lattice parameter which in the Nb case is $a=3.3008$ Å). The parameters A, d, c, c_0, c_1, and c_2 have been adjusted by FS in order to reproduce the following static properties: cohesion energy, lattice parameter, elasticity coefficient, and vacancy formation energy. The FS parameters are summarized in Table I.

However, the FS potential could not be used in MD simulations as it stands because the repulsive part of the potential is "too soft."[10,20] The system becomes unstable as soon as metal atoms are moved slightly from their equilibrium position. As a result, the dynamical crystal properties such as phonon frequency are not correctly reproduced. Gillan[10] has modified the repulsive part of the FS potential by replacing the polynomial form inside the nearest-neighbor distance by an exponential function. Such a modification allows us to get rid of the system instability in the MD simulations, but as it affects the attractive part of the potential the static properties of the Nb crystal cannot be reproduced. Starting with the FS potential, Ackland and Thetford[20] proposed an improved N-body semiempirical potential which overcomes the instability anomalies described above without changing the fit of static properties at the near equilibrium positions. This has been achieved by adding the term $h(r_{ij})$ to the pairwise part of the FS potential $V_{FS}(r_{ij})$ in order to increase the short-range repulsion:

$$V(r_{ij})=V_{FS}(r_{ij})+h(r_{ij}) \quad \text{for} \quad 0.4b_0<r_{ij}<b_0\ , \tag{8}$$

$$V(r_{ij})=V_{FS}(r_{ij}) \quad \text{for} \quad r_{ij}\geq b_0\ , \tag{9}$$

with

$$h(r_{ij})=B(b_0-r_{ij})^n e^{-\alpha r_{ij}}\ . \tag{10}$$

In the case of the Nb crystal, the distance b_0 to the nearest neighbor is equal to 2.8586 Å. The parameters B, n, and α have been adjusted to Ackland and Thetford in order to predict a realistic pressure-volume relationship. In the MD simulations of the Nb crystal we performed, the Ackland and Thetford potential has been adopted because, as we show in the next subsection, it leads to realistic dynamical properties of the Nb crystal. We have determined the values of the parameters B and α for the case of the Nb crystal by a minimization procedure.[14] Our values are close to those obtained by Ackland and Thetford, namely, $B=48.0$ eV Å^{-3}, $n=3$, and $\alpha=0.8$ Å^{-1}.

TABLE I. Parameters of the FS potential and experimental quantities to be fitted.

FS constants values
$d=3.915054$ Å
$c=4.20$ Å
$A=3.013789$ eV
$c_0=-1.56640104$
$c_1=2.0055779$
$c_2=-0.4663764$
Experimental data associated to static properties
Cohesive energy: $E_{coh}=7.57$ eV
Lattice parameter: $a=3.3008$ Å
Elastic constants: $C_{11}=2.46\times10^{11}$ Pa
$C_{12}=1.33\times10^{11}$ Pa
$C_{44}=1.18\times10^{11}$ Pa
Bulk modulus: $B=1.71\times10^{11}$ Pa
Surface energy: $\gamma_{100}=2.046$ J m^{-2}
Vacancy formation energy: $E_v^f=2.64$ eV

B. Dynamical properties of the Nb crystal

In our MD code the equations of motion of the system are solved in time steps using the Verlet leapfrog algorithm.[21,22] The classical dynamics approach was adopted which is adequate for temperatures greater than the Debye. The calculations were performed using a time step of 10^{-15} s. In each step, the number of atoms, volume, and total energy were kept constant (microcanonical ensemble). In this study of dynamical properties, the Nb crystal simulations included 1024 atoms.

MD simulations allow us to predict the variation of crystal internal pressure with lattice volume. The results are compared to experimental data[23] in Fig. 1, in which V_0 represents the volume of the elementary cell at thermodynamical equilibrium and temperature $T=300$ K. The agreement using the Ackland and Thetford potential is good up to high pressure values (1.2×10^6 bars), while using the FS potential the pressure-volume relation is not correctly reproduced.

Furthermore, we have fitted the experimental phonon dispersion curves of Nb. The phonon frequencies were measured by the technique of coherent inelastic neutron scattering and the experimental results used[24–26] were obtained at 300 K. Such data have been previously reproduced within a general tensor Born–von Karman phenomenological model. In our work, the phonon dispersion curve of niobium was extracted from the spectrum of the dynamical structure factor, $S(k,\omega)$. The factor $S(k,\omega)$ is the Fourier transform with respect to time of the correlation function, $F(k,t)$, of the density operator,

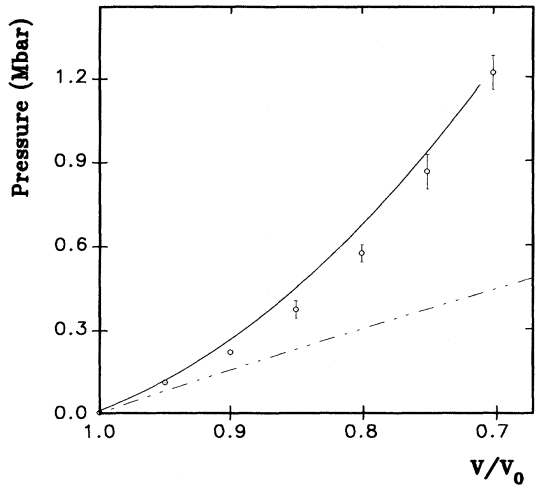

FIG. 1. Variation of the internal crystal pressure with lattice volume. MD simulations were performed with Ackland and Thetford potential (Ref. 18) (full line) and FS potential (Ref. 20) (dotted and dashed line). Experimental data (Ref. 23) are denoted by open circles.

$\rho_k(t)$,

$$\rho_k(t)=\sum_{j=1}^{N} e^{i\mathbf{k}\mathbf{r}_j(t)} , \tag{11}$$

where the sum is over N atoms of the system and $\mathbf{k}$ is the wave vector. The quantity $F(\mathbf{k},t)$ is given by

$$F(\mathbf{k},t)=\frac{1}{N}\langle \rho_k(t)\cdot\rho_{-k}(0)\rangle , \tag{12}$$

where the angular brackets denote a statistical average. The longitudinal phonon dispersion curve calculated in this way is given in Fig. 2. The simulation has been performed at 300 K. One can notice a good fit of the experimental data and especially of the anomalies along the directions $[\xi\xi\xi]$ and $[00\xi]$ of the longitudinal mode. However, the simulations are unable to reproduce the behavior of experimental data at the intersection of $[\xi\xi\xi]$ and $[00\xi]$ directions (point H) and they predict greater values at the upper end of the $[\xi\xi 0]$ direction (point N). Aiming to improve the agreement with experiment we introduced long-range interactions in the N-body potential as proposed by Eridon and Rao,[27] including the contribution of interactions with farther (up to five) atoms. This change allows us to adjust the maximum frequency of the phonons at the zones boundary H, but still the frequency modes in the middle of the ΓH region are not correctly reproduced. Taking into account a larger interaction range does not improve significantly the fit of experimental data, while it increases the computing time; therefore, we did not implement such calculations.

We tested the as-described Nb potential by calculating the variation of the mean-square displacement $\langle u^2\rangle$ of the Nb atom as a function of temperature. The projection on the x axis $\langle u_x^2\rangle$ is expressed as

$$\langle u_x^2\rangle=\langle (r_{x,i}(t)-\overline{r_{x,i}})^2\rangle_t , \tag{13}$$

where $r_{x,i}(t)$ is the x coordinate of the i atom at time t and $\overline{r_{x,i}}$ is its mean value (average on time). The MD simulations have been performed at 300, 800, 1000, and 1300 K (Fig. 3). In each case the Nb atoms' coordinates were recorded during the simulation time (10 ps) and $\langle u_x^2\rangle$ was calculated taking into account finite-size effect corrections.[29,30] We observed a vibrational isotropy in the three directions, $\langle u_x^2\rangle=\langle u_y^2\rangle=\langle u_z^2\rangle$, and a linear dependence of $\langle u_x^2\rangle$ with temperature as suggested in Fig. 3 by the dashed line. The experimental value of $\langle u_x^2\rangle$ can be obtained from the broadening of the Bragg peak due to thermal vibrations.[28] In the niobium case no data are available, but $\langle u_x^2\rangle$ can be deduced from the ex-

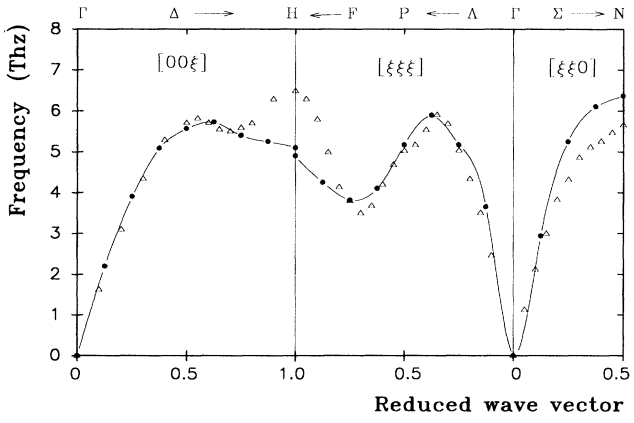

FIG. 2. Phonon dispersion curve calculated by the method of dynamical structure factor in the case of acoustical longitudinal mode, $[00\xi]$, $[\xi\xi\xi]$, and $[\xi\xi 0]$. Experimental values are represented by open triangles; the solid circles correspond to MD simulation. The line is only to guide the eyes.

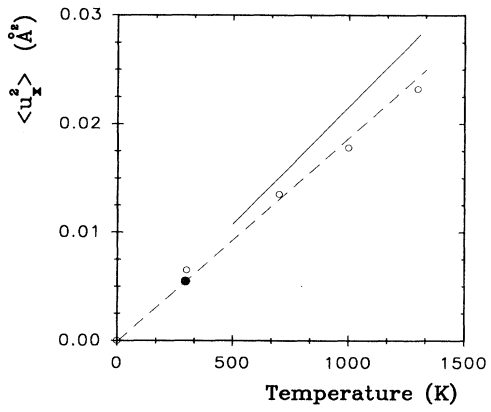

FIG. 3. Evolution of mean-square displacement with system temperature. (○) MD simulations. The dashed line is only to guide the eyes. (●) is obtained with Eq. (14) and phonon state density is measured at 300 K (Ref. 22). The full line was calculated with relation (15), which is only valid at high temperature.

perimental phonon density of state measurements $g(\omega)$. In the quasiharmonic approximation $\langle u_x^2 \rangle$ is written as

$$\langle u_x^2 \rangle = \frac{\hbar}{2M} \int_0^{\omega_{\max}} \frac{g(\omega)}{\omega} \coth \left[\frac{\hbar\omega}{2k_B T} \right] d\omega$$

$$\text{with} \quad \int_0^{\omega_{\max}} g(\omega) d\omega = 1 , \qquad (14)$$

where M is the mass of the niobium atom. One set of experimental data $g(\omega)$ obtained at $T=300$ K are available.[26] The value of $\langle u_x^2 \rangle$ thus obtained is shown by a black circle in Fig. 3. If the temperature is much greater than the Debye temperature ($T \gg \theta_D$) the integral of the quasiharmonic approximation can be reduced to the following expression:

$$\langle u_x^2 \rangle = \frac{3\hbar^2 T}{k_B \theta_D^2 M} . \qquad (15)$$

The mean-squared statistical values deduced within this classical approximation are represented in Fig. 3 by a continuous line for the 500 to 1300 K temperature range. The MD calculations reproduce the experimental result at 300 K and also predict correctly the behavior up to the high-temperature region ($T \gg \theta_D$). This entitles us to conclude that the Nb crystal simulation is adequate and can be used in the following.

III. MD SIMULATIONS OF HYDROGEN HOPPING IN THE Nb CRYSTAL

A. The model

Our work has been focused on the study of hydrogen diffusion in the bulk of the niobium crystal. Surface effects have not been considered. The calculation of a hydrogen trajectory in a crystal is determined by the interaction potential Nb-H. Fukai and Sugimoto[31] have proposed a two-term potential containing short- and long-range interactions. Simulations based on this potential gave a low activation energy, which is about half of the experimental value (experimental activation energy 101 meV, calculated value 61 meV). We assumed that the charge screening effect of the first-neighbor atoms is strong enough to hide the interaction between H and the second Nb neighbors. Therefore, we adopted an interaction potential with only one short-range term as proposed by Gillan,[10] that is,

$$V(r) = A \exp \left[-\frac{r}{\sigma} \right] . \qquad (16)$$

The parameters A and σ have been adjusted on a dynamical criterion basis, namely, by calculating the vibrational frequency[32] of H in the Nb crystal. The fit is shown in Fig. 4. It reproduces the two vibrations frequencies observed at 26.5 THz and 43.4 THz due to the tetrahedral site symmetry of the bcc Nb crystal. Such agreement has been obtained by setting the parameters A and σ equal to 25000 eV and 0.16 Å, respectively.

In order to avoid the trapping of more than one of the H atoms in the tetrahedral (T) sites, which would produce a lattice deformation and restrict the diffusion, we introduced a Lennard-Jones H-H potential and adopted the parametrization given by Murad and Gubbins.[33] Because the van der Waals energies are small compared to the amplitude of thermal vibrations in the crystal, the inclusion of the H-H potential does not alter the dynamics of the system, but it prevents multihydrogen trapping in the same T sites.

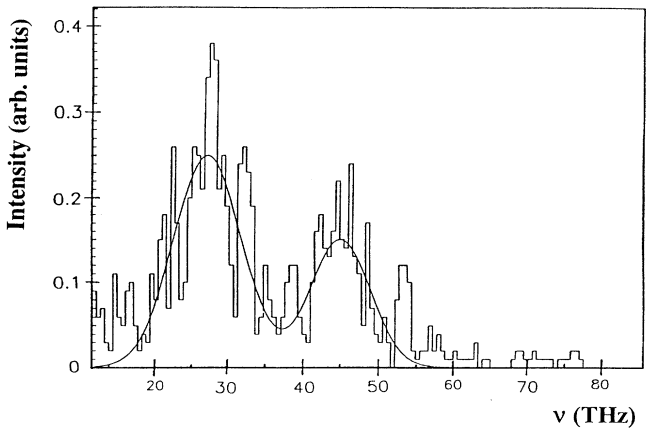

FIG. 4. Histogram of hydrogen vibration frequency in Nb deduced from MD simulations, fitted by two Gaussians (continuous line).

B. Simulation and analysis of H jumps

In order to reproduce the experimental conditions (i.e., H concentration of few atomic per cent in Nb), we randomly introduced four hydrogen atoms in different T sites of the 432 Nb simulated crystal. The initial velocities for all atoms are assigned stochastically according to a Gaussian distribution while the total momentum of the system is kept at zero. During the simulation run the hydrogen coordinates were recorded at each time increment (in steps of 10^{-15} s). A typical H trajectory projected on a {100} plane is shown in Fig. 5, in which only tetrahedral sites, octahedral sites, and niobium sites located in the plane are drawn. Such a plot clearly shows that hydrogen atoms spend most of their time in T sites, inside the {100} plane as well as outside this plane; this has also been observed in channeling experiments.[34,35] Moreover, we want to point out a typical result of MD simulations. When jumping from one T site to another, the hydrogen atom does not go through the saddle point S (as static equipotential calculations would predict), but a little bit further at S' due to crystal relaxation. The distance SS' is nearly equal to one-third of the distance between the saddle point and the octahedral site. Such behavior has been previously observed by Gillan[10] in a quasistatic calculation.

Examination of this trajectory step by step gives information on the correlation character in the H hopping process. We performed a simulation of hydrogen hopping in a niobium crystal at various temperatures 250,

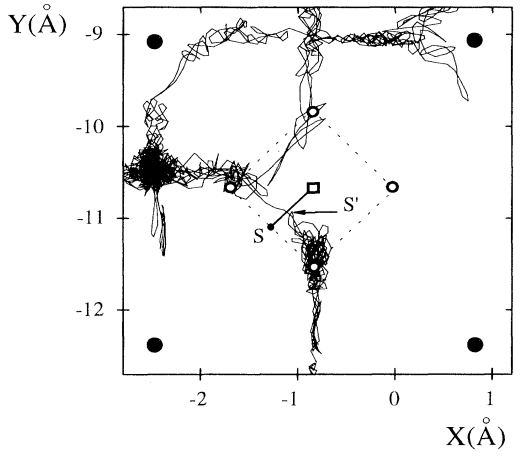

FIG. 5. Trajectory of a hydrogen atom at temperature 300 K projected into the {100} plane. Solid circles correspond to positions of Nb atoms in the nonrelaxed configuration. Open circles and squares indicate tetrahedral and octahedral sites, respectively, while S is the saddle point, located at midpoint between two first-neighboring tetrahedral sites.

300, 600, and 1000 K, in which H hopping is restricted to the nearest-neighbor sites. Whatever the temperature is, the successive transitions between T sites are the most probable; they represent 97% of the jumps observed at 250 K. Transitions involving octahedral sites are very few. Let us focus on jumps between T sites. Figure 6 shows that the jump angles θ (defined as the angle between the directions of two successive jumps) are equal to $\pi/3$, $\pi/2$, and π. In the case of random distributions, the probabilities corresponding to hydrogen jumping at an angle of $\pi/3$, $\pi/2$, and π in a bcc crystal are equal to 0.5, 0.25, and 0.25, respectively. In MD simulations the H behavior is not random at all. As shown in Fig. 7, π angle jumps are very much favored; for example, at $T=250$

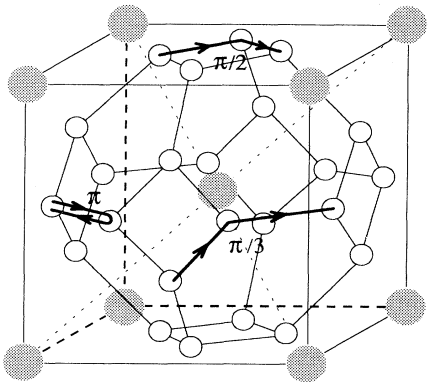

FIG. 6. Representation of different kinds of jumps between successive T sites. The grey circles represent Nb atoms. The open circles denote tetrahedral sites. Jump angles are represented by black arrows.

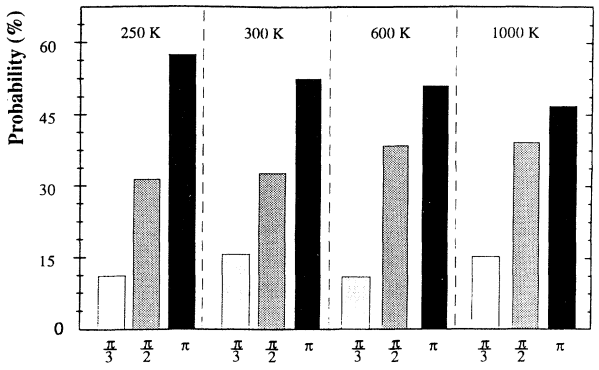

FIG. 7. Angle probability distributions of jumps between T sites. The simulation box contains 432 Nb and 4 H. For each temperature the simulation time is equal to 20 ps.

K they are 55% π jumps instead of 25% in the random case. One possible explanation of such a strong correlation effect is the following: the nth T site where the H was previously sitting is not completely relaxed when H is jumping from the $(n+1)$th T site. Therefore, in making a π jump, the H atom prefers to return to the nth T site which is favored because of lattice deformations. Discrepancy with random behavior is also observed in the case of $\pi/3$ and $\pi/2$ jumps. For the case of $T=250$ K mentioned above, the MD simulations predict, respectively, 13% and 34% probability values instead of 50% and 25%. Jumps at the angle $\pi/3$ are less probable, while jumps at the angle $\pi/2$ are enhanced, which corresponds to easier H diffusion along the {100}, {010}, or {001} planes. As shown in Fig. 7 the lattice influence becomes less important when temperature is increased, but it still persists even when reaching 1000 K. In order to put on a quantitative basis such dynamical effects we need to define two parameters. The mean time between two jumps, τ_L, is deduced from an MD calculation by dividing the simulation time by the number of jumps. If τ_S is the time of flight of a hydrogen atom of mass m, when moving along the distance δ in an ideal gas at a temperature T, it can be expressed using Boltzman theory as $\tau_S=\delta\sqrt{m/3k_BT}$. The results presented in Fig. 8 have

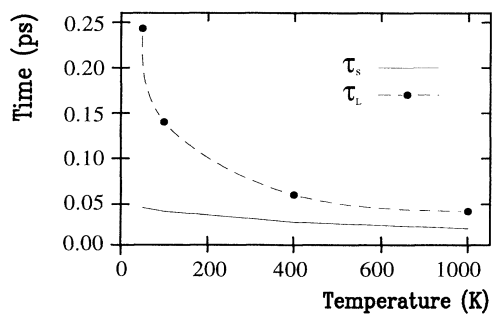

FIG. 8. Mean time τ_L between two successive jumps of H and time of flight τ_S versus temperature.

been obtained setting δ equal to the distance to the nearest neighbor in a Nb crystal ($\delta=2.8586$ Å). One sees in Fig. 8 that at low temperature, τ_L is much larger than τ_S, while they become comparable at temperatures close to 1000 K. This can be explained by the fact that at low temperature, H is trapped in the T site for a time longer than the transit time. Therefore, τ_L, which includes both transit time and the time spent in the T site, is much larger than τ_S. At high temperatures, H is trapped for a negligible time: as soon as H reaches the T site it starts the next jump, thus behaving like a "fluid." This analysis of hydrogen jumping in the Nb crystal is used in the study of the diffusion process presented in the next section.

IV. HYDROGEN DIFFUSION IN NIOBIUM CRYSTAL

The temperature dependence of the diffusion coefficient D of hydrogen in niobium has been measured by many groups and a collection of data is presented in Ref. 6. The data show that D has an Arrhenius form in the temperature range 250 K $< T <$ 1000 K, and a fit to the data gives us a value for the activation energy, $\Delta E_a=0.11$ eV. However, experimental data[36–38] show the influence of defects on the diffusion coefficient values. In order to investigate such effects, we first present simulations of H diffusion in a perfect Nb crystal and compare the results to those obtained in an imperfect crystal.

A. Diffusion in a single crystal

The diffusion coefficient can be obtained by evaluating the time-dependent displacement of hydrogen, $\langle \Delta r(t)^2 \rangle$, defined as

$$\langle \Delta r(t)^2 \rangle = \frac{1}{N} \sum_{i=1}^{N} \langle |\mathbf{r}_i(t)-\mathbf{r}_i(o)|^2 \rangle \ , \tag{17}$$

where $\mathbf{r}_i$ denotes vector positions of the H atom and N the number of H atoms. In the infinite time limit[22] the diffusion coefficient D is given by

$$D=\frac{1}{6t}\langle \Delta r(t)^2 \rangle \ . \tag{18}$$

The diffusion coefficient can also be obtained by evaluating the jump frequency Γ, which is the inverse of the mean time, τ_L, between two jumps. Assuming a random behavior of hydrogen atoms as proposed in Ref. 39, one can deduce the following relation:

$$D=\frac{\Gamma a^2}{48} f \ , \tag{19}$$

where a is the lattice parameter in the bcc crystal. The correlation coefficient f allows us to take into account the nonrandom behavior of hydrogen atoms. $f=1+\langle \cos\theta \rangle$, where θ is the angle defined above related to two successive jumps.

Using both methods, we can calculate the diffusion coefficient of H in a niobium crystal (432 atoms) at temperatures ranging from 250 to 1000 K (Table II). As previously observed by Gillan at high temperature,[10] the computational diffusion coefficient obeys the Arrhenius law within statistical errors. One can notice that hydrogen diffusion coefficients calculated using either the time-dependent displacement or jump frequency range in the same order of magnitude. The important result is the fact that both sets of values shown in Table II lead to the same activation energy value $\Delta E_a=0.07$ eV, which is lower than the activation energy ($\Delta E_a=0.11$ eV) deduced from experimental data.[6]

In order to investigate the influence of defects on diffusion constants we performed MD simulations of H diffusion in a crystal containing a vacancy and in a bicrystal.

B. Diffusion in an imperfect crystal

We first consider the influence of a vacancy on hydrogen migration. Our approach is similar to experimental procedure[39] in which defects have to be created artificially to study their effects on dynamical properties. In fact, the manufacturing process for niobium semifinished products (tubes, sheets) involves electron-beam melting of pure niobium and additional hot and cold working techniques. Such techniques as well as irradiation processes are known to create defects with high concentration. The simulations are performed for a 432 Nb crystal in which one vacancy is created by removing one Nb atom. The N-body potential allows us to take into account the atomic rearrangement in the neighborhood of the vacancy. Previously performed simulations[40] yield a decrease in the distance from the vacancy to the nearest neighbor by 2.5%, and an increase of 2% of the distance to the next nearest neighbors. Such an effect destroys the crystal symmetry; therefore, the simulation cell must be large enough in order to avoid interactions between vacancies, as well as interactions between atoms along the edge of the simulation box. The 432 site simulation box corresponds to such criteria and therefore the Born-von Karman conditions are respected. Furthermore, the monovacancy formation energy for niobium, determined from positron annihilation measurements[41,42] appears to be 2.65 eV. FS monovacancy formation energy (see Table I) is very close to the measured one. Thus

TABLE II. Hydrogen diffusion coefficient (D) calculated using hydrogen displacement and jump frequency. Diffusion coefficients are given in $cm^2\,s^{-1}$.

Temperature	1000 K	610 K	415 K	310 K	240 K
D (displacement)	2.1×10^{-4}	1.2×10^{-4}	6.5×10^{-5}	3.5×10^{-5}	2.5×10^{-6}
D (jump frequency)	3.0×10^{-4}	2.0×10^{-4}	1.0×10^{-4}	7.5×10^{-5}	4.0×10^{-5}

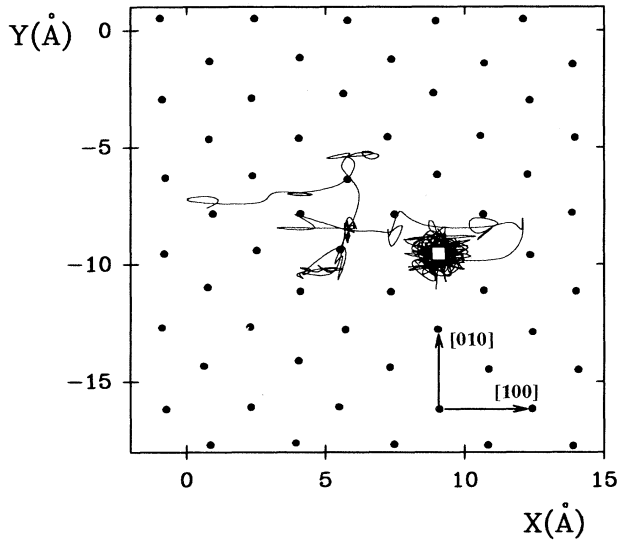

FIG. 9. Trapping of hydrogen in a monovacancy crystal at $T=300$ K. The simulation time is equal to 35 ps. Solid circles correspond to positions of Nb atoms in the nonrelaxed configuration. The location of the vacancy is indicated by the open square.

in the temperature range we are working (300–1000 K) the vacancy formation enthalpy is much larger than the thermal vibration energy and niobium autodiffusion cannot occur. The system is in a steady state even though its vacancy concentration of 0.2 at. % is orders of magnitude larger than the one at thermal equilibrium. In this steady system, four hydrogen atoms are introduced far away from the vacancy site. The H trapping in the vacancy site is clearly shown in Fig. 9. The diffusion coefficient deduced from hydrogen displacement is given in Table III together with experimental data. The agreement of simulations to experiment is good; the activation energy value deduced from these data is equal to 0.11 eV in both the simulated and experimental cases.

Let us now consider the case of a grain boundary on a bicrystal. Such features have been used by several authors[43,44] in order to study grain-boundary properties in metal. The system chosen in our simulation is a $\Sigma=5$ coincidence site lattice tilt boundary in the bcc niobium crystal. It is generated by a rotation of 36°89′ along the $\langle 001 \rangle$ axis. The bicrystal is represented in Fig. 10 by its projection on the (x,y) plane; seven periods of the coincidence site boundary are shown with atoms forming

TABLE III. Comparison of experimental data and diffusion coefficients deduced from hydrogen displacement in the case of a monovacancy single-crystal simulation. Diffusion coefficients are given in $cm^2 s^{-1}$.

Temperature	1000 K	600 K	450 K	300 K
D (simulation)	1.7×10^{-4}	6.1×10^{-5}	3.0×10^{-5}	1.5×10^{-5}
D (experiment)	1.5×10^{-4}	6.0×10^{-5}	3.0×10^{-5}	1.2×10^{-5}

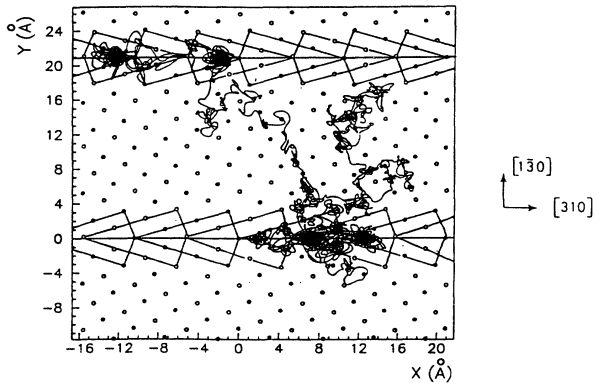

FIG. 10. Hydrogen trajectory simulation at $T=1300$ K in a bicrystal model of a $\Sigma=5$ tilt boundary. The simulation time is equal to 200 ps.

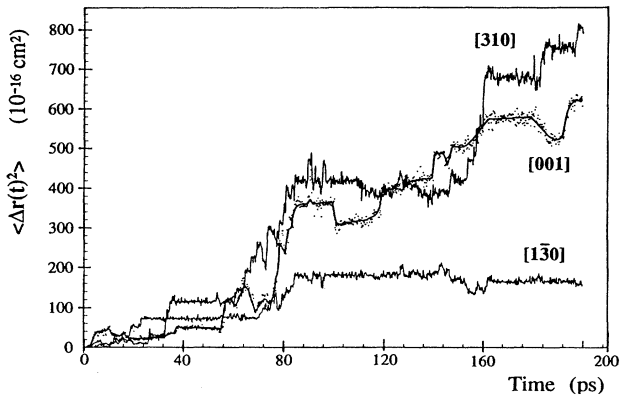

FIG. 11. Displacement of H along the main bicrystal axes [310], [1$\bar{3}$0], and [001].

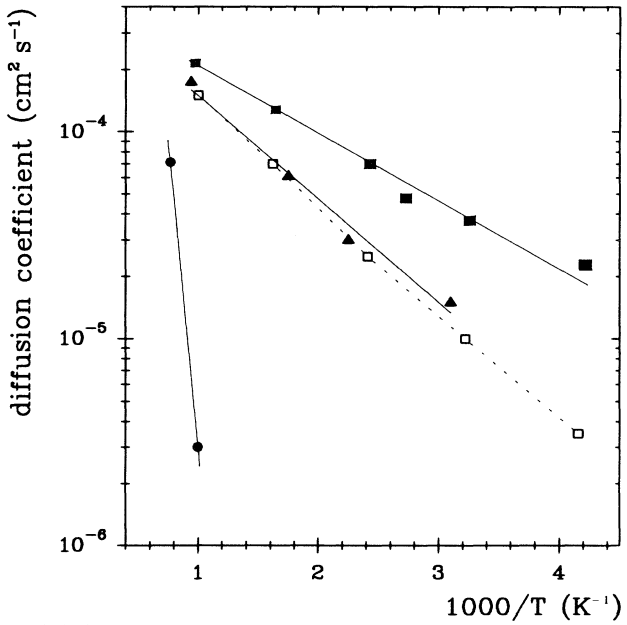

FIG. 12. Diffusion coefficient of H in Nb. Experimental data are denoted by open squares. MD simulations are represented by solid squares in the case of a single crystal, by solid triangles after a vacancy creation, and by solid circles in the case of a bicrystal ($\Sigma=5$).

kitelike figures occupying the lattice sites in the grain-boundary core regions. Because of periodic boundary conditions, another bicrystal is generated at the edge of the simulation box. In order to avoid interactions between grain boundaries, a large number of atomic planes are needed. The simulation system is a stack of 480 atoms, placed in a noncubic box, whose dimensions are $L_x = L_y = 20.62$ Å and $L_z = 9.9$ Å. Using such a configuration, we allowed the system to relax and we checked that the mean positions of Nb atoms in the intermediate zone (between the two grain-boundary regions) were close to those observed in a perfect crystal. In order to simulate H diffusion, four hydrogen atoms are introduced far away from the grain boundary. The hydrogen trajectories represented in Fig. 10 show evidence of H trapping in the grain boundary. The lowest potential energy is in the middle of the coincidence site lattice between the two crystals, which explains the strong H trapping observed. Furthermore, the hydrogen displacement given in Fig. 11 shows that H propagation along the $[1\bar{3}0]$ axis perpendicular to the bicrystal is disadvantaged. We performed calculations at temperatures of 1300 and 800 K, respectively, and the deduced H diffusion coefficients are presented in Fig. 12. One should be careful in ascribing to the calculated diffusion coefficient values an absolute quantitative significance, because of the limitations due to inadequacies in the potential function and possible nonphysical effects introduced by finite system size and insufficient statistical sampling. But evidence of an increase in activation energy due to lattice defects is clearly seen in Fig. 12, by the change in the slope of the temperature dependence of the diffusion coefficients. Furthermore, around 1000 K the diffusion coefficient values reach the same order of magnitude whatever the crystal conditions are. Such results support the empirically established need of heating rf superconducting cavities to 1000 K in a UHV furnace, in order to remove hydrogen contamination and consequently recover good superconducting properties.

V. CONCLUSIONS

In this work, MD computer simulation was used to study the predominant localization sites and migration paths of hydrogen in the bcc niobium lattice. Interesting characteristics of hydrogen diffusion in Nb have emerged in the case of an imperfect crystal. We have considered a microcrystallite in the form of a cube with periodic boundary conditions that contains 432 niobium atoms. The N-body Nb-Nb potential used in the simulations has been determined for describing the static and dynamic properties of the Nb crystal. To simulate the few percent interstitial H in niobium sheets that causes drastic changes in superconducting performances of high-frequency cavities, four H atoms are introduced in the simulation cell. Diffusion of hydrogen in a perfect crystal is compared to the case of diffusion in an imperfect crystal. The comparisons show evidence of strong hydrogen trapping at defects. MD was used to calculate the diffusion coefficient of hydrogen in niobium for crystal temperatures in the 250 to 1000 K range. It is only around 1000 K that the diffusion of hydrogen is not altered by defects. This conclusion confirms the experimental results concerning good properties (Q value $> 10^{10}$) of superconducting cavities after thermal treatments.

*Permanent address: Department of Chemistry, SUNY-Stony Brook, NY 11790.

[1]B. Aune and P. Leconte, Nucl. Phys. News **1**(2), 19 (1990).
[2]B. Bonin and R. W. Röth, Part. Accel. **40**, 59 (1992).
[3]R. M. Röth, H. Heinrichs, V. G. Kurakin, G. Muller, H. Piel, J. Pouryamont, in *Proceedings of the 2nd European Accelerator Conference, Nice, 1990* (Frontière, Nice, 1990), p. 1097.
[4]S. Isigawa, J. Appl. Phys. **51**, 4460 (1980).
[5]C. K. Khaldeev and V. K. Gogel, Russian Chem. Rev. **56**, 605 (1987).
[6]J. Völkl and G. Alefeld, in *Hydrogen in Metal I,* edited by G. Alefeld and J. Völkl (Springer, Berlin, 1978), p. 330.
[7]R. J. Hempelmann, J. Less-Common. Met. **101**, 69 (1984).
[8]J. A. Rodrigues and R. Kirchheim, Scr. Metall. **17**, 159 (1983).
[9]Y. Fukai and H. Sugimoto, Adv. Phys. **34**, 263 (1985).
[10]M. J. Gillan, Phys. Rev. Lett. **58**, 313 (1987).
[11]M. J. Gillan, Philos. Mag. A **58**, 257 (1988).
[12]J. W. Culvahouse and P. M. Richards, Phys. Rev. B **38**, 10 020 (1988).
[13]Y. Li and G. Wahnström, Phys. Rev. B **46**, 14 528 (1992).
[14]B. Roux, Ph.D. thesis, Université Claude Bernard Lyon-1, 1993.
[15]J. Friedel, in *The Physics of Models,* edited by J. M. Ziman (Pergamon, London, 1969), p. 340.
[16]F. Ducastelle, J. Phys. (Paris) **31**, 1055 (1970).
[17]F. Ducastelle, in *Computer Simulation in Materials Science,* Vol. 205 of NATO ASI Series B, edited by M. Meyer and V. Pontikis (Kluwer Academic, Dordrecht, 1991), p. 223.
[18]M. W. Finnis and J. E. Sinclair, Philos. Mag. A **50**, 6443 (1984).
[19]M. S. Daw and M. I. Baskes, Phys. Rev. B **29**, 6443 (1984).
[20]G. J. Ackland and R. Thetford, Philos. Mag. A **56**, 15 (1987).
[21]L. Verlet, Phys. Rev. **159**, 98 (1967).
[22]M. P. Allen and D. J. Tildeslay, *Computer Simulation of Liquids* (Clarendon, Oxford, 1987).
[23]K. W. Katahara and M. H. Manghanani, J. Appl. Phys. **47**, 434 (1976).
[24]Y. Nakagawa and A. D. B. Woods, Phys. Rev. Lett. **11**, 271 (1963).
[25]B. M. Powel, P. Martel, and A. D. B. Woods, Phys. Rev. **171**, 727 (1963).
[26]J. Sharp, J. Phys. C **2**, 421 (1969).
[27]J. Eridon and S. Rao, Philos. Mag. Lett. **59**, 31 (1989).
[28]C. J. Martin and D. A. O'Connor, J. Phys. C **10**, 3521 (1977).
[29]V. Rosato, M. Guillope, and B. Legrand, Philos. Mag. A **59**, 321 (1989).
[30]F. Willaime, Ph.D. thesis, Université Paris-Sud, 1991.
[31]Y. Fukai and H. Sugimoto, Phys. Rev. B **22**, 670 (1980).
[32]T. Springer, in *Hydrogen in Metal I* (Ref. 6), p. 75.
[33]S. Murad and K. E. Gubbins, in *Computer Modeling of*

Matter, edited by P. Lykos, ACS Symposium Series Vol. 86 (American Chemical Society, Washington, 1978), p. 62.
[34]H. D. Carstanjen, Phys. Status Solidi A **59**, 11 (1980).
[35]S. T. Picraux, Nucl. Instrum. Methods **182/183**, 413 (1981).
[36]A. D. Leclaire, Ann. Chim. (Paris) **14**, 93 (1989).
[37]C. K. Khaldeev and V. K. Gogel, Russ. Chem. Rev. **56**, 1057 (1987).
[38]T. Mutochele and R. Kirchheim, Scr. Metall. **21**, 137 (1987).
[39]J. Philibert, *Diffusion et Transport de Matiére dans les Solides* (Editions de Physique, Paris 1985).
[40]C. C. Matthai and D. J. Bacon, Philos. Mag. A **52**, 1 (1985).
[41]M. Suezawa and H. Kimura, Philos. Mag. **28**, 901 (1973).
[42]H. E. Schaeffer, in *Proceedings of the Sixth International Conference on Positron Annihilation, Arlington, 1982,* edited by P. C. Coleman and S. C. Sharma (North-Holland, Amsterdam, 1982), p. 369.
[43]K. Kwok, P. S. Ho, and S. Trip, Phys. Rev. B **29**, 5354 (1984); **29**, 5363 (1984).
[44]C. Goux, J. Phys. (Paris) Colloq. **36**, C4-111 (1975).